

# Statistical Distribution of Charge Carriers in $\beta$ -HgS Quantized Layer in Lateral Electrostatic Field

Volodya Harutyunyan<sup>1</sup>

<sup>1</sup>Russian-Armenian University  
123, H.Emin st., Yerevan, 0051, Republic of Armenia  
Volodya.harutyunyan@rau.am

**Abstract**—The specificity of the statistical distribution of electrons, heavy and light holes in a plane-parallel metacinnabar film under conditions of a quantum size effect and in the presence of a transversal electrostatic field is considered in the effective mass approximation. Consideration was carried out for the case when only the first film subband of size quantization is filled. Explicit analytical expressions are obtained for the chemical potential and concentration, internal energy, and heat capacity of the electron-hole subsystem in the quantized film in the absence and presence of an external field. The analysis of the dependence of the indicated statistical characteristics of the material on the quantizing thickness of the layer, the strength of the external field and temperature of the system is carried out. The corresponding numerical estimates are also given.

**Keywords:** size quantization, charge carriers, electrostatic field, chemical potential, concentration, energy

## 1. Introduction

In recent decades, various semiconductor nanostructures based on metacinnabar (mercury sulfide  $\beta$ -HgS modification) have been studied intensively [1-6]. Currently, they have wide applications and are used in various electronic and optoelectronic devices with low energy consumption [7-8], in solar and photoelectrochemical batteries [3,9,10], as a promising material for the implementation of new quantum states in solids - excitonic insulators [3,11,12], in modern biomedicine [4,13-15], ecology [13-15], etc.

Among the aforementioned semiconductor nanomaterials, a separate place is occupied by semiconductor structures with planar symmetry based on  $\beta$ -HgS quantum films. The size-quantized thin films of  $\beta$ -HgS [16, 17] are currently used, for example, in the creation of infrared detectors, photoconductors, elements of memory cells, for the creation of highly efficient thin-film solar cells [18-21] etc. In the case of planar symmetry (as in the cases of quantized films with axial [22] and spherical symmetry [1, 23]), size quantization of charge carriers in the  $\beta$ -HgS layer is often achieved by placing a layer of narrow-band  $\beta$ -HgS (band gap  $E_g = 0,5$  eV [1, 24 -26]) between two layers of wide-gap semiconductor  $\beta$ -CdS (band gap  $E_g = 2,5$  eV [1, 24-26]). The choice of cadmium sulfide as “plates” is primarily due to the similarity of the type of crystal lattices (both types of zinc blende) and very close values of the lattice constant ( $a$ ) of the contacting materials [24–26]:  $a_{CdS} = 0,5818$  nm,  $a_{HgS} = 0,5851$  nm.

As in any semiconductor, in  $\beta$ -HgS also a number of the most important physical properties are determined by the statistical distribution of charge carriers. On the other hand, it is known that dimensional quantization and external electrostatic field are powerful modulating factors that make it possible to control the physical characteristics of the sample. In this paper, we consider theoretically the effects of lateral external electrostatic field on the statistical distribution of charge carriers in the quantum layer  $\beta$ -HgS of the planar  $\beta$ -CdS /  $\beta$ -HgS /  $\beta$ -CdS heterostructure.

## 2. Influence of size quantization on the statistical distribution of charge carriers in the $\beta$ -HgS quantum layer of a planar heterostructure $\beta$ -CdS / $\beta$ -HgS / $\beta$ -CdS

Table 1 shows the further necessary physical characteristics of bulk crystals of  $\beta$ -CdS and  $\beta$ -HgS.

Table 1. Some characteristics of bulk semiconductors  $\beta$ -CdS and  $\beta$ -HgS (Data taken from Refs. [22-27]).

Material	Electron eff. mass $m_e/m_0$	Light hole eff. mass $m_{lh}/m_0$	Heavy hole eff. mass $m_{hh}/m_0$	Electron affinity $U_c$ (eV)	Bandgap $E_g$ (eV)	Light exciton bound energy $E_{e-lh}^{3D}$ (meV)	Heavy exciton bound energy $E_{e-hh}^{3D}$ (meV)	Light exciton Bohr rad. $a_{e-lh}^{3D}$ (nm)	Heavy exciton Bohr rad. $a_{e-hh}^{3D}$ (nm)
CdS	0.2	0.7	5	-3.8	2.5	27	32	3	2.5
HgS	0.036	0.044	0.31	-5	0.5	0.81	1.32	50	30

Here  $m_0$  is the free electron mass

It is clear from the data presented that due to the large value of the energy offset ( $\Delta U_{c,v}$ ) at the interface of contacting materials ( $\Delta U_c = 1,2 \text{ eV}$  for  $c$ -band and  $\Delta U_v = 0,8 \text{ eV}$  for  $v$ -band, respectively), in the direction of growth of the heterostructure, we will have a heterojunction of the first kind. In this heterojunction, the HgS layer acts as a quantum well, and the CdS layers act as barriers. Because we are interested in the statistical distribution of the "pure" charge carriers; it is natural that their size quantization must be considered in the strong quantization regime, when exciton effects can be neglected in the quantized HgS layer. The Coulomb interaction in the direction of growth of the heterostructure can be neglected when the size quantization energy of carriers is greater than the energy of their Coulomb interaction, i.e., when the condition

$$L^2 \ll (a_{ex}^{3D})^2 \quad (1)$$

takes place. Here  $L$  is the thickness of the HgS layer,  $a_{ex}^{3D}$  - is the Bohr radius of 3D exciton in bulk  $\beta$ -HgS crystal. It is easy to conclude from Table 1 that for a layer thickness  $L=5 - 20 \text{ nm}$ , the condition (1) will be satisfied with sufficient accuracy. Accordingly, for the energies of size quantization of charge carriers ( $E_{e, lh, hh}^{conf}$ ) in the  $\beta$ -HgS layer, we will have:

$$E_e^{conf} \sim \frac{\hbar^2}{2m_e L^2} = 42,39 - 2,65 \text{ meV}; E_{lh}^{conf} \sim \frac{\hbar^2}{2m_{lh} L^2} = 34,68 - 2,17 \text{ meV}; E_{hh}^{conf} \sim \frac{\hbar^2}{2m_{hh} L^2} = 4,93 - 0,31 \text{ meV} \quad (2)$$

Here  $\hbar$  is Planck constant. Comparing the values of the dimensional quantization energies (2) - (4) with the values of  $\Delta U_c = 1,2 \text{ eV}$ ,  $\Delta U_v = 0,8 \text{ eV}$ , it is easy to verify that, in order to calculate the energy of the fundamental level of size quantization, which is of greatest physical interest, in the direction of structure growth ( $z$ ), the  $\beta$ -HgS layer can be approximated with high accuracy by an infinitely deep rectangular potential well [28,29]. Accordingly, the energy spectrum ( $E_i^1(\vec{p}); \vec{p} = \vec{p}(p_x, p_y, 0)$ ) of charge carriers for the ground level in the  $\beta$ -HgS quantized layer of the heterostructure under considered can be written in the following form [28, 29]:

$$E_i^1(\vec{p}) = (E_i^{conf})_1 + \frac{\vec{p}^2}{2m_i} = \frac{\pi^2 \hbar^2}{2m_i L^2} + \frac{\vec{p}^2}{2m_i}; \quad (i = e, lh, hh; \vec{p} = \vec{p}(p_x, p_y, 0)) \quad (3)$$

For the manifestation of size quantization in  $\beta$ -HgS layer (when only the first subband is filled), the following conditions is imposed on the temperature and concentration ( $\rho_e$ ) of the system [29]:

$$k_B T < (E_i^{conf})_2 - (E_i^{conf})_1 = \frac{3\pi^2 \hbar^2}{2m_i L^2}; \quad \rho_e < \frac{2 \cdot 2\pi m_e}{(2\pi \hbar)^2 L} \int_{(E_e^{conf})_1}^{(E_e^{conf})_2} dE = \frac{3\pi}{2L^3}; \quad (4)$$

Here  $k_B$  is Boltzmann constant. For an intrinsic semiconductor, the fulfillment of this condition simultaneously implies that the number of electrons in the conduction band should be less than the number of states in the first film subband:

For a fixed value of  $L$ , the smallest value of the size quantization energy is the quantization energy of a heavy hole. Accordingly, for a given  $L$  in the  $\beta$ -HgS quantized layer, the quantum size effect will take place for all types of charge carriers at temperatures

$$T < T_0^{hh}(L) = 3\pi^2 \hbar^2 / 2k_B m_{hh} L^2; T_0^{hh}(L = 5nm) \approx 1752K, T_0^{hh}(L = 10nm) \approx 438K, T_0^{hh}(L = 20nm) \approx 110K \quad (5)$$

In particular:  $T_0^{hh}(L = 5nm) \approx 1752K, T_0^{hh}(L = 10nm) \approx 438K, T_0^{hh}(L = 20nm) \approx 110K$ .

Let us now proceed to calculating the statistical characteristics of equilibrium charge carriers in the  $\beta$ -HgS layer in the absence of an external field.

## 2.1. Chemical potential

Provided that only the first size quantization subband is filled, we can write the following expressions for the concentrations of electrons ( $\rho_e(T, L)$ ), light ( $\rho_{lh}(T, L)$ ) and heavy holes ( $\rho_{hh}(T, L)$ ):

$$\rho_e(T, L) = \frac{4\pi m_e}{(2\pi\hbar)^2 L} \int_{(E_e^{conf})_1}^{\infty} \left[ \exp\left(\frac{E_e^1(p) - \mu}{k_B T}\right) + 1 \right]^{-1} dE_e^1; \left( E_e^1(p) = (E_e^{conf})_1 + \frac{p^2}{2m_e} \right) \quad (6)$$

$$\rho_{lh}(T, L) = \frac{4\pi m_{lh}}{(2\pi\hbar)^2 L} \int_{(E_{lh}^{conf})_1}^{\infty} \left[ \exp\left(\frac{E_{lh}^1(p) + E_g + \mu}{k_B T}\right) + 1 \right]^{-1} dE_{lh}^1; \left( E_{lh}^1(p) = (E_{lh}^{conf})_1 + \frac{p^2}{2m_{lh}} \right) \quad (7)$$

$$\rho_{hh}(T, L) = \frac{4\pi m_{hh}}{(2\pi\hbar)^2 L} \int_{(E_{hh}^{conf})_1}^{\infty} \left[ \exp\left(\frac{E_{hh}^1(p) + E_g + \mu}{k_B T}\right) + 1 \right]^{-1} dE_{hh}^1; \left( E_{hh}^1(p) = (E_{hh}^{conf})_1 + \frac{p^2}{2m_{hh}} \right) \quad (8)$$

Here  $\mu$  is chemical potential of the system. Integrals (6)-(8) are calculated exactly and from the electroneutrality condition

$$\rho_e(T, L) = \rho_{lh}(T, L) + \rho_{hh}(T, L) \quad (9)$$

for the chemical potential  $\mu(T, L)$  of electrons and holes of intrinsic non-degenerate semiconductor we obtain:

$$\mu(T, L) = -\frac{E_g}{2} + \frac{(E_e^{conf})_1 - (E_{hh}^{conf})_1}{2} + \frac{k_B T}{2} \ln \frac{m_{hh}}{m_e} + \frac{k_B T}{2} \frac{m_{lh}}{m_{hh}} \exp\left[-\frac{(E_{lh}^{conf})_1 - (E_{hh}^{conf})_1}{k_B T}\right] \quad (10)$$

As is known, in the case of a bulk intrinsic semiconductor the chemical potential of the system is located in the middle of the band gap at absolute zero, In a quantum layer-film, at  $T = 0$ , the chemical potential shifts upward from the middle of the band gap towards the conduction band by an amount

$$\Delta\mu(T = 0) = 1/2 \left( (E_e^{conf})_1 - (E_{hh}^{conf})_1 \right) \sim 1/L^2 \quad (11)$$

At a nonzero temperature, the chemical potential starting from its minimum value for a given layer thickness increases linearly with increasing of sample temperature. The magnitude of the displacement is determined by the layer thickness and decreases with increasing of  $L$ , tending to zero in the limit  $L \rightarrow 0$ . In addition, it can be seen from expression (10) that in the formation of the position of the chemical potential of the quantum layer, from the carriers of the valence band, the dominant role is played by heavy holes. Physically, this can be explained by the fact that with the energy levels of heavy holes are located closer to the band gap than the quantization levels of light holes.

## 2.2. Concentration of charge carriers

Substituting now Exp.(10) into Exps. (6) - (8), for the concentrations of electrons and holes in absence of external field we obtain:

$$\rho_e(T, L) = \frac{(m_e m_{hh})^{1/2} k_B T}{\pi \hbar^2 L} \exp \left[ -\frac{E_g + (E_e^{conf})_1 + (E_{hh}^{conf})_1}{2k_B T} \right] \cdot \exp \left[ \frac{m_{lh}}{2m_{hh}} e^{-\frac{(E_e^{conf})_1 - (E_{hh}^{conf})_1}{k_B T}} \right] \quad (12)$$

$$\rho_{hh}(T, L) = \rho_e(T, L) \exp \left[ -\frac{m_{lh}}{m_{hh}} e^{-\frac{(E_e^{conf})_1 - (E_{hh}^{conf})_1}{k_B T}} \right]; \quad \rho_{lh}(T, L) = \rho_{hh}(T, L) \frac{m_{lh}}{m_{hh}} \exp \left[ -\frac{(E_{lh}^{conf})_1 - (E_{hh}^{conf})_1}{k_B T} \right] \quad (13)$$

Thus, the concentration of light holes in is exponentially smaller then the concentration of heavy holes. This is due to the fact that the size quantization energy of heavy hole is much less than the size quantization energy of a light hole.

Table 2 shows the values of electron density ( $\rho_e$ ,  $\text{cm}^{-3}$ ) in the conduction band at a layer thickness of  $L = 5, 10, 15$  nm for various values ( $T = 200-500\text{K}$ ) of the system's temperature.

Table2. Values of electron density at a layer thickness of  $L = 5, 10, 15$  nm for various values of the system's temperature.

$T$ (K)	200K	250K	300K	350K	400K	450K	500K
$L$ (nm)	$\rho_e(T, L)$ $\text{cm}^{-3}$	$\rho_e(T, L)$ $\text{cm}^{-3}$	$\rho_e(T, L)$ $\text{cm}^{-3}$	$\rho_e(T, L)$ $\text{cm}^{-3}$	$\rho_e(T, L)$ $\text{cm}^{-3}$	$\rho_e(T, L)$ $\text{cm}^{-3}$	$\rho_e(T, L)$ $\text{cm}^{-3}$
5 nm	$5 \cdot 10^5$	$2 \cdot 10^8$	$1,1 \cdot 10^{10}$	$5 \cdot 10^{11}$	$2 \cdot 10^{12}$	$1,1 \cdot 10^{13}$	$4,3 \cdot 10^{13}$
10 nm	$8,3 \cdot 10^9$	$4,2 \cdot 10^{11}$	$6 \cdot 10^{12}$	$4,1 \cdot 10^{13}$	$1,8 \cdot 10^{14}$	$5,6 \cdot 10^{14}$	$1,4 \cdot 10^{15}$
15 nm	$4,4 \cdot 10^{10}$	$1,4 \cdot 10^{12}$	$1,5 \cdot 10^{13}$	$8,6 \cdot 10^{13}$	$3,5 \cdot 10^{14}$	$9,1 \cdot 10^{14}$	$2,1 \cdot 10^{15}$

The data presented in the table show that at a fixed film thickness, the density of free electrons in the conduction band increases with increasing temperature. This is due to an increase in the value of the energy of thermal motion, due to which the number of transitions from the valence band to the conduction band increases. On the other hand, at a fixed temperature, the electron concentration increases with increasing of film thickness. As in the case of the carriers' concentration (Exps. (12) - (13)), the determining factor for determining the carriers' energy, along with the film thickness, is the band gap of the material.

## 2.3. Energy and heat capacity of electron-hole system in the layer

Taking into account expressions (10) and (12) - (13) for the volume density of the energy ( $\varepsilon_{e,th,hh}(T, L)$ ) of carriers' subsystems, we obtain, respectively:

$$\varepsilon_e(T, L) = \rho_e(T, L) \left[ k_B T + (E_e^{conf}(L))_1 \right] \quad (14)$$

$$\varepsilon_{lh}(T, L) = \rho_{lh}(T, L) \left[ k_B T + E_g + (E_{lh}^{conf}(L))_1 \right]; \quad \varepsilon_{hh}(T, L) = \rho_{hh}(T, L) \left[ k_B T + E_g + (E_{hh}^{conf}(L))_1 \right] \quad (15)$$

Analysis of expressions (14), (15) shows that with increasing of temperature, the internal energy of the carrier subsystems increases. This is due to an increase in the amount of transferred heat energy. The internal energy of electrons and hole in the layer increases also with an increase of the thickness of the quantizing layer. This is due to an increase in the number of particles in it with an increase of the layer's thickness.

Table 3 shows the values of internal energy of electrons in the conduction band at a layer thickness of  $L = 5, 10, 15$  nm for various values ( $T = 200-500\text{K}$ ) of the system's temperature.

Table 3. Values of internal energy of electrons at a layer thickness of  $L = 5, 10, 15$  nm for various values of the system's temperature.

$T(K)$	200K	250K	300K	350K	400K	450K	500K
$L(nm)$	$\varepsilon_e(T, L)$ -3 J/cm	$\varepsilon_e(T, L)$ -3 J/cm	$\varepsilon_e(T, L)$ -3 J/cm	$\varepsilon_e(T, L)$ -3 J/cm	$\varepsilon_e(T, L)$ -3 J/cm	$\varepsilon_e(T, L)$ -3 J/cm	$\varepsilon_e(T, L)$ -3 J/cm
5nm	$3,5 \cdot 10^{-14}$	$1,4 \cdot 10^{-11}$	$7,8 \cdot 10^{-10}$	$1,4 \cdot 10^{-8}$	$1,5 \cdot 10^{-7}$	$8 \cdot 10^{-7}$	$3,2 \cdot 10^{-6}$
10nm	$1,6 \cdot 10^{-10}$	$8,5 \cdot 10^{-9}$	$1,3 \cdot 10^{-7}$	$8,9 \cdot 10^{-7}$	$4 \cdot 10^{-6}$	$1,2 \cdot 10^{-5}$	$3,3 \cdot 10^{-5}$
15nm	$4,4 \cdot 10^{-10}$	$1,5 \cdot 10^{-8}$	$1,7 \cdot 10^{-7}$	$1 \cdot 10^{-6}$	$4,5 \cdot 10^{-6}$	$1,3 \cdot 10^{-5}$	$2,9 \cdot 10^{-5}$

Accordingly, for the specific heat capacity ( $C_{e, lh, hh}(T, L)$ ) of carriers' subsystems we get out, respectively:

$$C_e(T, L) = \frac{\partial \varepsilon_e}{\partial T} = \left[ k_B T + (E_e^{conf})_1 \right] \frac{\partial \rho_e}{\partial T} + k_B \rho_e \quad (16)$$

$$C_{lh}(T, L) = \frac{\partial \varepsilon_{lh}}{\partial T} = \left[ k_B T + E_g + (E_{lh}^{conf})_1 \right] \frac{\partial \rho_{lh}}{\partial T} + k_B \rho_{lh}; \quad (17)$$

$$C_{hh}(T, L) = \frac{\partial \varepsilon_{hh}}{\partial T} = \left[ k_B T + E_g + (E_{hh}^{conf})_1 \right] \frac{\partial \rho_{hh}}{\partial T} + k_B \rho_{hh}$$

Analysis shows that the specific capacity of charge carriers at low temperatures is close to zero, but increases with increasing of temperature. Figure 1 shows the temperature dependence of electronic heat capacity  $C_e(T)$  for the film thickness  $L = 5, 10, 15$  nm.

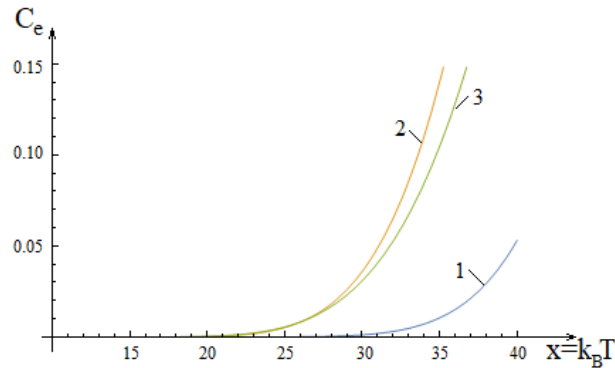


Fig.1. Curves of the dependence of the electronic heat capacity (Exp.16) on temperature  $x = k_B T \in [15; 50]$  meV for the values of film thickness  $L = 5(1), 10(2), 15(3)$  nm.

### 3. Influence of lateral electrostatic field on the statistical distribution of charge carriers in the $\beta$ -HgS quantum layer of a planar heterostructure $\beta$ -CdS / $\beta$ -HgS / $\beta$ -CdS

Let us now consider the effect of transverse to the layer external electrostatic field  $F = F(0, 0, F)$  on statistical characteristics of charge carriers in  $\beta$ -HgS layer. As we know, an external electrostatic field leads to a narrowing of the semiconductor band gap by some value  $\Delta E_g(F)$  [28-31]. To calculate the statistical characteristics of the material in the presence of an external field it is necessary to carry out a formal replacement

$$E_g \rightarrow E'_g(F) = E_g - \Delta E_g(F) \quad (18)$$

in all previous calculations. Accordingly, in the presence of an external field, instead of (10) and (12)- (17) we get:

$$\mu' \equiv \mu'(T, L, F) = \mu(T, L) + \Delta E_g(F)/2; \rho'_i \equiv \rho'_i(T, L, F) = \rho_i(T, L) \exp[\Delta E_g(F)/2k_B T]; \quad (i = e, lh, hh) \quad (19)$$

$$\varepsilon'_e \equiv \varepsilon'_e(T, L, F) = \rho'_e(T, L, F) \left[ k_B T + (E_e^{conf}(L))_1 \right] \quad (20)$$

$$\varepsilon'_{lh} \equiv \varepsilon'_{lh}(T, L, F) = \rho'_{lh}(T, L, F) \left[ k_B T + E'_g(F) + (E_{lh}^{conf}(L))_1 \right] \quad (21)$$

$$\varepsilon'_{hh} \equiv \varepsilon'_{hh}(T, L, F) = \rho'_{hh}(T, L, F) \left[ k_B T + E'_g(F) + (E_{hh}^{conf}(L))_1 \right] \quad (22)$$

$$C'_e \equiv C'_e(T, F) = \frac{\partial \varepsilon'_e}{\partial T} = \left[ k_B T + (E_e^{conf})_1 \right] \frac{\partial \rho'_e}{\partial T} + k_B \rho'_e \quad (23)$$

$$C'_{lh} \equiv C'_{lh}(T, F) = \frac{\partial \varepsilon'_{lh}}{\partial T} = \left[ k_B T + E'_g(F) + (E_{lh}^{conf})_1 \right] \frac{\partial \rho'_{lh}}{\partial T} + k_B \rho'_{lh} \quad (24)$$

$$C'_{hh} \equiv C'_{hh}(T, F) = \frac{\partial \varepsilon'_{hh}}{\partial T} = \left[ k_B T + E'_g(F) + (E_{hh}^{conf})_1 \right] \frac{\partial \rho'_{hh}}{\partial T} + k_B \rho'_{hh} \quad (25)$$

The sign ( $\varepsilon'$ ) means that energy and all characteristics are calculated in the presence of an external field. To carry out specific calculations of the dependence of the statistical characteristics of  $\beta$ -HgS on the external field, it is necessary to estimate the degree of influence of a field with a given strength on the band gap of the sample. So, all of the above is true for the fields whose strength is limited by the following condition:

$$|e|FL < E_g/2 \quad (26)$$

For the strength values  $F > F_0 = E_g/2|e|L_B$  in the sample, there will already be possible the horizontal interband transitions through tunneling. Taking such phenomena into account is beyond the physical scope of this consideration. Based on the quantum confined Stark effect [28,30,31] we arrive at the following estimate: than the intensity of the external field is in the interval

$$|e|FL \square 2(E_{hh}^{conf})_1; \Delta E_g(F, L) \approx -0,11(eFL)^2 / (E_{hh}^{conf})_1 \quad (27)$$

the external field can be taken into account as a perturbation for all types of charge carriers in the layer. When  $|e|FL > (E_{hh}^{conf})_1$ , the external field can no longer be regarded as a perturbation for heavy holes. Taking into account that  $m_e \approx m_{lh}$ , the external field can be considered as a perturbation for light holes and electrons, up to values

$$|e|FL \square 2(E_e^{conf})_1; \Delta E_g(F, L) \approx -0,11(eFL)^2 / (E_e^{conf})_1 \quad (28)$$

With a further increase in the field strength, the condition (26) must be met. In this case, the perturbation theory is no longer applicable and other calculation methods must be applied [28 - 31].

#### 4. Conclusion

Regarding the modulating effect of dimensional quantization and an external electrostatic field on the statistical characteristics of the structure under consideration, we can conclude the following:

– Under the influence of size quantization, the position of the chemical potential at  $T = 0$  in comparison with the bulk sample is shifted upward to the bottom of the conduction band. The magnitude of the displacement is determined by the

energy of the ground level of the dimensional quantization of charge carriers. From the valence band, only heavy holes contribute to this displacement.

– Under the action of an external field, an effective narrowing of the band gap of the quantized  $\beta$ -HgS layer occurs. This leads to an additional upward shift of the position of the chemical potential at  $T=0$ . The magnitude of this displacement is determined by the strength of the external field and the width of the quantum well of the layer.

– In the absence of an external field at a fixed film thickness, the carriers' concentration increases with increasing temperature. On the other hand, at a fixed temperature the carrier concentration increases with increasing film thickness.

– A similar behavior is also manifested by the internal energy of the electron-hole subsystem in the layer.

– The specific heat capacity of the carriers increases with temperature. Moreover, the smaller the thickness of the quantizing layer, the lower the temperature values from which a significant increase in heat capacity begins.

– The imposition of an external field leads to an increase of the carriers' concentration. At a fixed film thickness and system temperature, the carriers' concentration in the layer increases with an increase of the external field's strength. Accordingly, the presence of an external field leads to an increase in the internal energy and heat capacity of the sample.

Summarizing the results of the work, it can be argued that by varying the geometric dimensions of the sample and the magnitude of the external field in the allowable intervals, it is possible to achieve a controlled change in the statistical characteristics of the quantized  $\beta$ -HgS layer.

## Acknowledgment

This work was financially supported by the Horizon-2020 research and innovation program of the European Union (grant no. 952335, NanoQIQO project).

## References

- [1] D. Schoos, A. Mews, A. Eychemüller, and H. Weller, "Quantum-dot quantum well CdS/HgS/CdS: Theory and experiment", *Phys. Rev. B*, vol. 49, no. 24, pp.17072–17078, 1994.
- [2] A. Rogach, *Semiconductor Nanocrystal Quantum Dots: Synthesis, Assembly, Spectroscopy and Applications*, Springer, 2008.
- [3] X. Xu, E. R. Carraway, "Sonication-Assisted Synthesis of  $\beta$ -Mercuric Sulphide Nanoparticles", *Nanomater. and Nanotechnol.*, vol. 2, Art. no.17:2012, pp.1-6, 2012.
- [4] K.M. F. Joy, N. V. Jaya, "Electrical resistivity of Nano-HgS under high pressure and temperature", *Journ. Chem. Pharm. Sci.*, vol.9, no. 4, pp. 2387-2390, 2016.
- [5] K. Liu, G.Gao, T.Sun, " $\beta$ - HgS Quantum Dots: Preparation, Properties and Applications", *Progr. in Chem.*, vol. 29, no.7, pp.776-784, 2017.
- [6] J.O. Akinlami, F.C. Onyeonu, "Electronic and optical properties of  $\beta$ -HgS", *SPQEO*, vol. 22, no.2, pp.150-155, 2019.
- [7] W.Wichiansee, M. N. Nordin, M. Green, R. J. Curry, "Synthesis and optical characterization of infra-red emitting mercury sulfide (HgS) quantum dots", *J. Mater. Chem.*, vol. 21, no.20, pp.7331-7336, 2011.
- [8] J. Kim, B. Yoon, J. Kim, Y. Choi, Y.-W. Kwon, S. K. Park, K. S. Jeong, "High electron mobility of  $\beta$ -HgS colloidal quantum dots with doubly occupied quantum states", *RSC Adv.*, vol. 7, no. 61, pp. 38166 – 38170, 2017.
- [9] I. Galain, I. Aguiar, M. Eugenia, P. Barthaburu, L. Fornaro, "First steps to use  $\beta$ -HgS nanostructures in solution as electron acceptor in organic/inorganic solar cells", in *Proceedings of XIV Brazil MRS Meeting - Rio de Janeiro*, p.99, 2015.
- [10] M. Barthaburu, I. Galain, A.H.B. Pereira, L. Bethencourt, P.B. Miranda, M.F.B. Sampaio, L. Fornaro, "Hybrid  $\beta$ -HgS nanoparticles and P3HT layers for solar cells applications", *Nano-Struct. & Nano-Objects*, vol., 10, pp.15-21, 2017.
- [11] G.G. Roberts, E.L. Lind, E.A. Davis, "Photoelectronic Properties of Synthetic Mercury Sulphide Crystals", *J. Phys. Chem. Solids*, vol. 30, pp.833 - 844, 1969.
- [12] F. Virost, R. Hayn, M. Richter, J. van den Brink, "Metacinnabar ( $\beta$  - HgS): A Strong 3D Topological Insulator with Highly Anisotropic Surface States", *Phys. Rev. Letter.*, vol. 106, no. 23, pp.236806 - 1 - 4, 2011.

- [13] S. Rajendran, *Metal, metal oxides and metal sulfides for biomedical applications*, Springer Nature, 2020.
- [14] F. Yang, G. Gao, J. Wang, R. Chen, W. Zhu, L. Wang, Z. Ma, Z. Luo, T. Sun, "Chiral  $\beta$ -HgS quantum dots: Aqueous synthesis, optical properties and cytocompatibility", *J. Colloid. Interface Sci.*, vol. 573, pp. 422-430, 2019.
- [15] N. J. Mohammed, H. F. Dagher, "Synthesis and Characterization of Mercuric Sulfide Nanoparticles Thin Films by Pulsed Laser Ablation (PLA) in Distilled Water (DW)", *Iranian Journ. Mater. Sci. & Eng.*, vol. 17, no.3, pp.11-16, 2020.
- [16] K.R. Sanadi, P.D.Sanadi, M.L.Gaur, G.S.Kamble, "Optical, electrical and morphological studies of  $\beta$ -HgS thin film prepared by improved chemical bath deposition technique", *Bull. Mater. Sci.* vol. 44, no. 1, art.42, pp.42-1-42-5, 2021.
- [17] L. Geng, Zh. Xia, L. Yuan, C. Li, M. Zhang, Y. Du, L. Wei, H. Bi, "Effects of  $\beta$ -HgS on cell viability and intracellular oxidative stress in PC-12 cells", *Metallomics*, v.12, no. 9, pp.1389-1399, 2020.
- [18] J. Mu, Y. Zhang, Y. Wang, "Growth and Characterization of  $\beta$ -HgS Thin Films by Annealing  $\text{Hg}^{2+}$ -Dithiol Self-Assembled Multilayers", *J. Disp. Sci. Technol.*, vol. 26, no.5, pp.641-644, 2005.
- [19] V. E. Stadnik, M. A. Sozanskyi, N. M. Koval, P. Y. Shapoval, Y. Y. Yatchyshyn, "Hydrochemical synthesis and properties of mercury (II) sulphide and mercury (II) selenide films. Review", *SCHMT (Series of chemistry, materials technology and their Application)*, v.886, pp.3-13, 2018.
- [20] M.E.P. Barthaburu, I. Galain, I. Aguiar, H. B. Pereira, L. Bethencourt, P. B. Miranda, M. F.B. Sampaio, L. Fornaro, "Hybrid -HgS nanoparticles and P3HT layers for solar cells applications", *Nano-Struct. & Nano-Objects*, vol.10, pp.15-21, 2017.
- [21] A. Rahul, R.A. Wagh, A.N. Kulkarni, P.K.Baviskar, H.M. Pathan, R.S. Patil "Fabrication of titanium dioxide ( $\text{TiO}_2$ ) and mercury sulfide (HgS) heterojunction for photoelectrochemical study", *Mater Renew Sustain Energy*, vol.7, Art. no.13, 2018.
- [22] V.A. Harutyunyan, D.B. Hayrapetyan, E.M. Kazaryan, "Optical Transitions and Photoluminescence in Cylindrical Core/Layer/Shell  $\beta$ -CdS/ $\beta$ -HgS/ $\beta$ -CdS Heterostructure", *Phys. Sol. St.*, vol. 62, no. 8, pp. 1305–1316, 2020.
- [23] V.A. Harutyunyan, "Optical transitions in semiconductor nanospherical layer under the presence of perturbing electrical field", *Phys. E*, vol. 39, pp. 37-49, 2007
- [24] V.A. Harutyunyan, D. B. Hayrapetyan, D. A. Baghdasaryan, "Single-Electron States in Semiconductor Nanospherical Layer of Large Radius", *Journ. Contem. Phys. (Armenian Academy of Sciences)*, vol. 51, no. 4, pp. 350–359, 2016.
- [25] V. A. Harutyunyan, D. B. Hayrapetyan, E. M. Kazaryan, "Interband Absorption and Photoluminescence in the Cylindrical Layered CdS/HgS/CdS Heterostructure", *Journ. Contemp. Phys. (Armenian Academy of Sciences)*, vol. 53, no. 1, pp. 48–57, 2018.
- [26] O. Madelung, *Semiconductor Data Handbook*, 3-rd ed., Springer, 2004.
- [27] F. Benhaddou, a I. Zorkani, A. Jorio, "The confinement effect in spherical inhomogeneous quantum dots and stability of excitons", *AIP Advances*, vol 7, pp. 065112-1-6, 2017.
- [28] VA Harutyunyan, *Effect of Static Electric Fields on the Electronic and Optical Properties of Layered Semiconductor Nanostructures*, Chapter 1, Bentham Science, 2015.
- [29] V.A. Harutyunyan, "Statistics of charge carriers of quantum semiconductor film in the presence of strong lateral electrostatic field", *AIMS Mater. Sci.*, vol.5, no. 2, pp.257–275, 2018.
- [30] D.A.B. Miller, D.S. Chemla, T.C. Damen, A.C. Gossard, W. Weigman, T.H. Wood, C.A. Burrus, "Band-edge electroabsorption in quantum well structure: the quantum confined Stark effect", *Phys. Rev. Lett.*, vol. 53, no.22, pp.2173- 2176, 1984.
- [31] J. Faist, *Optical Properties of Semiconductors*, Zurich, 2008.